NEOPLASIA
www.neoplasia.com

Volume 13 Number 7 July 2011 pp. 590–600 590

Modulation of the Unfolded Protein Response Is the Core of MicroRNA-122–Involved Sensitivity to Chemotherapy in Hepatocellular Carcinoma[1,2]

Fu Yang[3], Ling Zhang[3], Fang Wang, Yue Wang, Xi-song Huo, Yi-xuan Yin, Yu-qi Wang, Lin Zhang and Shu-han Sun

Department of Medical Genetics, the Second Military Medical University, Shanghai, China

Abstract

The loss of microRNA-122 (miR-122) expression correlates to many characteristic properties of hepatocellular carcinoma (HCC) cells, including clonogenic survival, anchorage-independent growth, migration, invasion, epithelial-mesenchymal transition, and tumorigenesis. However, all of these findings do not sufficiently explain the oncogenic potential of miR-122. In the current study, we used two-dimensional differential in-gel electrophoresis to measure changes in the expression of thousands of proteins in response to the inhibition of miR-122 in human hepatoma cells. Several proteins that were upregulated on miR-122 inhibition were involved in the unfolded protein response (UPR) pathway. The overexpression of miR-122 resulted in the repression of UPR pathway activation. Therefore, miR-122 may act as an inhibitor of the chaperone gene expression and negatively regulate the UPR pathway in HCC. We further showed that the miR-122 inhibitor enhanced the stability of the 26S proteasome non-ATPase regulatory subunit 10 (PSMD10) through the up-regulation of its target gene cyclin-dependent kinase 4 (CDK4). This process may activate the UPR pathway to prevent chemotherapy-mediated tumor cell apoptosis. The current study suggests that miR-122 negatively regulates the UPR through the CDK4-PSMD10 pathway. The down-regulation of miR-122 activated the CDK4-PSMD10-UPR pathway to decrease tumor cell anticancer drug–mediated apoptosis. We identified a new HCC therapeutic target and proclaimed the potential risk of the therapeutic use of miR-122 silencing.

Neoplasia (2011) 13, 590–600

Introduction

The endoplasmic reticulum (ER) is the cellular site of synthesis of secretory and membrane proteins. These proteins must be properly folded, which requires the aid of the molecular chaperone proteins [1,2]. Stress that is caused by hypoxia, nutrient deprivation, or chemotherapy can lead to an excess of unfolded protein in the ER lumen of tumor cells. Tumor cells respond to these stresses by activating the unfolded protein response (UPR), which is a series of signaling cascades that restore a favorable folding environment. Recent data suggest that UPR plays a key role in protecting cancer cells from an inadequate environment and, therefore, contributes to tumor growth and survival [3–5].

Hepatocellular carcinoma (HCC) is one of the most prevalent malignancies and is a leading cause of cancer death worldwide. Eighty percent of newly developed HCC cases occur in developing countries; however, the incidence of HCC has increased steadily, particularly in western countries [6,7]. Despite successful local therapies such as surgery and transcatheter arterial chemoembolization, patients with HCC develop a high rate of recurrence and metastasis [8]. Some studies have shown a link between UPR activation and poor clinical outcomes, and high levels of UPR chaperone expression correlate to an increasing tumor grade in HCC [6,7]. Furthermore,

Abbreviations: miRNA, microRNA; ER, endoplasmic reticulum; PSMD10, proteasome 26S subunit, non-ATPase, 10; CDK4, cyclin-dependent kinase 4; UPR, unfolded protein response; GRP78, glucose-regulated protein 78; HCC, hepatocellular carcinoma; DOX, doxorubicin

Address all correspondence to: Shu-han Sun, PhD, MD, or Fang Wang, PhD, MD, Department of Medical Genetics, The Second Military Medical University, Xiang Yin Road 800, Shanghai 200433, China. E-mail: shsun@vip.sina.com, wfsjz70@gmail.com

[1]This research was supported by a grant from the Major State Basic Research Development Program of China (973 Program; no. 2006CB504100).

[2]This article refers to supplementary materials, which are designated by Tables W1 and W2 and Figure W1 and are available online at www.neoplasia.com.

[3]These two authors contributed equally to this work.

Received 18 March 2011; Revised 28 April 2011; Accepted 29 April 2011

DOI 10.1593/neo.11422

in vitro activation of the UPR pathway alters the sensitivity of tumor cells to chemotherapeutic agents [4,8]. Oncoprotein proteasome 26S subunit non-ATPase 10 (PSMD10), which is consistently overexpressed in HCC [9,10], enhances the activation of the UPR pathway to promote tumor growth and inhibit apoptosis in HCC cells [11]. Therefore, understanding UPR pathway activation is of basic and clinical significance to the treatment of HCC.

The microRNAs (miRNAs) play an important role in the control of numerous biological processes [12–14]. Growing evidence indicates that miRNAs have a significant role in tumor development and may constitute robust biomarkers for cancer diagnosis and prognosis [18–21]. MicroRNA-122 (miR-122) is the most abundant miRNA in the liver, accounting for approximately 70% of the total miRNA population [15]. Several studies have emphasized the importance of miR-122 in liver homeostasis [16]. The expression of miR-122 is high in mouse and human hepatocytes but is either silent or very low in most HCC and transformed cell lines [17–19]. The loss of miR-122 expression correlates to hepatic differentiation phenotype, invasion, and intrahepatic metastasis [19–21]. More recently, the tumor suppressor and drug sensitization properties of miR-122 were defined *in vitro* and *in vivo* using nude mice [22,23]. A previous study demonstrated that miR-122 influenced the sensitivity of HCC cells to doxorubicin (DOX) through a p53-independent apoptosis pathway [23]. However, the detailed mechanism by which this phenomenon occurs remains unknown. Those previous findings do not sufficiently explain the oncogenic potential of miR-122. New techniques and approaches are required to study the complex functions of miR-122.

A proteomic approach was successfully used to examine the global impact of miRNAs on protein output [24,25]. In our current study, we silenced miR-122 in Huh7 cells, which express a relatively high level of miR-122 [26]. Differential proteomics results showed that the inhibition of miR-122 in hepatoma cells resulted in the up-regulation of several molecules involved in the UPR pathway. Importantly, we detected the up-regulation of PSMD10 in Huh7 cells that were transfected with the miR-122 inhibitor. PSMD10 has been shown to promote recovery from ER stress by upregulating the glucose-regulated protein 78 (GRP78) and, therefore, may enhance the ER protein folding capacity in Huh7 cells [11]. Considering the key role of the UPR pathway in tumor biology [4,27], we performed a thorough mechanistic study of the regulation of the UPR by miR-122. Our findings suggest that the ability of miR-122 to alter tumorigenic properties is at least partly based on its negative regulation of the UPR pathway.

Materials and Methods

Cell Culture, Treatment, Protein Expression Analysis, and Viability Assay

Huh7 and HepG2 cells were maintained in modified Eagle medium and Dulbecco modified Eagle medium, respectively, which were supplemented with 10% fetal calf serum (Gibco, Grand Island, NY) at 37°C in 5% CO_2. Huh7 cells were transiently transfected with the miR-122 inhibitor (Dharmacon, Lafayette, CO) or negative control RNAs using Lipofectamine 2000 (Invitrogen, Carlsbad, CA) following the manufacturer's protocol. After 48 hours, the cells were harvested for the miR-122 quantitative analysis, the proteomic experiments, or the Western blot assay. Expression of miR-122 was analyzed using the TaqMan MicroRNA Assay (Applied Biosystems, Foster City, CA) according to the manufacturer's protocol.

Two-dimensional differential in-gel electrophoresis (DIGE), image analysis, and protein identification were performed as previously described [25,28].

To assess the cells' sensitivity to cisplatin (Sigma-Aldrich, St Louis, MO) or DOX (Tocris Bioscience, Ellisville, MO), cell numbers were evaluated using a Cell Counting Kit (CCK) 8 (Dojindo, Kumamoto, Japan) as previously described [28].

Western Blot Analysis and Quantitative Real-time Polymerase Chain Reaction

Transfected cells were washed twice with phosphate-buffered saline, resuspended in sample buffer (50 mM Tris-HCl, pH 8.0, 150 mM NaCl, 0.02% NaN_3, 100 μg/L of phenylmethylsulfonyl fluoride, 1 μg/ml of aprotinin, and 1% Triton X-100) and allowed to lyse on ice for 30 minutes. The lysates were then centrifuged at 16,000*g* for 30 minutes at 4°C. Protein samples were separated using sodium dodecyl sulfate–polyacrylamide gel electrophoresis in 12% polyacrylamide gels and transferred onto nitrocellulose membranes (Amersham Biosciences, Uppsala, Sweden). The membranes were then blocked with nonfat milk and incubated with a 1:5000 dilution of mouse monoclonal antiactin (Sigma-Aldrich) or 1:500 dilutions of goat anti-PSMD10, GRP78, or mouse anticalreticulin (CALR), ER protein 29 (ERP29), phospho–eukaryotic initiation factor 2 α subunit (p-eIF2α), eIF2α, phospho–inositol-requiring enzyme-1α (p-IRE1α), IRE1α, and cleaved caspase 3 (Santa Cruz Biotechnology, Inc, Santa Cruz, CA). Membranes were then incubated with 1:10000 dilutions of Irdy680-conjugated goat antimouse IgG or Irdy800-conjugated rabbit antigoat IgG, and the bands were detected using an Odyssey infrared scanner (Li-COR, Lincoln, NE).

The total RNA was isolated from cells using the TRIzol reagent (Invitrogen) and was reverse-transcribed using SuperScript II reverse transcriptase and random hexamers (Invitrogen) according to the manufacturer's instructions. Subsequently, complementary DNA was subjected to quantitative real-time polymerase chain reaction (PCR) using gene-specific primers (Table W1) and StepOne Plus Real-Time PCR System (Applied Biosystems) following the manufacturer's protocol.

Plasmid Structure, Small Interfering RNAs, and Ectopic Expression of miR-122 Plasmid Structure

The human pre–miR-122 gene expression plasmid was purchased from GeneCopoeia (Guangzhou, China). Briefly, the precursor miRNA expression clone (pEZX–miR-122) was constructed using the vector pEZX-MR01. The pEZX-MR01 plasmid was used as an empty vector control. The transcription of the hairpin precursor was driven by an RNA polymerase III–type promoter. This vector allows for processing of precursor miRNAs (approximately 150 nucleotides in length) to generate mature miRNAs using the enzymes involved in the RNAi machinery. The antibiotic resistance gene was used to select the stable cell line for further experiments. Stable HCC cell cultures expressing miR-122 were generated by transfection with the pEZX–miR-122 plasmid followed by antibiotic selection (800 μg/ml of neomycin) for 2 weeks. Stable expression of mature miR-122 was confirmed using the TaqMan MicroRNA Assay (Applied Biosystems).

The human miR-122 inhibitor expression plasmid (miRZip 122) was purchased from System Biosciences (San Francisco, CA). Briefly, the miRZip short hairpin RNAs were cloned into the SBI's pGreenPuro shRNA expression lentivector. The miRZip hairpins were designed to be asymmetrical such that the upper strand of the hairpin does

not contain the endogenous microRNA sequence, and the lower strand is preferred for producing antisense microRNAs that are fully complementary to miR-122. The pGreenPuro shRNA expression lentivector was used as an empty vector control.

To construct an RNAi expression vector for human PSMD10 (PLKO-shPSMD10), the following oligonucleotides were ligated into the *Age*I-*Eco*RI site downstream of the U6 promoter of PLKO.1puro: oligo1 encoding human PSMD10 shRNA1 (shRNA-58073, an annealed mixture of two DNA oligomers: forward, 5′CCGGTCCGATAAATCCCTGGCTACTACTCGAGTAGTAGCCAGGGATTTATCGGTTTTTG3′; and reverse, 5′AATTCAAAAACCGATAAATCCCTGGCTACTACTCGAGTAGTAGCCAGGGATTTATCGGA3′), oligo2 encoding human PSMD10 shRNA2 (shRNA-58074, an annealed mixture of two DNA oligomers: forward, 5′CCGGTGCTCAAGTGAATGCTGTCAATCTCGAGATTGACAGCATTCACTTGAGCTTTTTG3′; and reverse, 5′AATTCAAAAAGCTCAAGTGAATGCTGTCAATCTCGAGATTGACAGCATTCACTTGAGCA3′) and oligo3 encoding human PSMD10 shRNA3 (shRNA-58076, an annealed mixture of two DNA oligomers: forward, 5′CCGGTCCAGTGAATGATAAAGACGATCTCGAGATCGTCTTTATCATTCACTGGTTTTTG3′; and reverse, 5′AATTCAAAAACCAGTGAATGATAAAGACGATCTCGAGATCGTCTTTATCATTCACTGGA 3′). The PLKO.1puro plasmid was used as an empty vector control.

As previously described [10], the small interfering RNA (siRNA) that specifically targeted PSMD10 (sense strand 5′-GACACUGAGGGUAACACUCCUU-3′, antisense strand 5′GGAGUGUUACCCUCCAGUGUCUU-3′), cyclin-dependent kinase 4 (CDK4; sense strand 5′-AGAUUACUUUGCUGCCUUATT-3′, antisense strand 5′ UAAGGCAGCAAAGUAAUCUCT-3′), and control siRNAs (sense strand: 5′-GACCCGCGCCGAGGUGAAGTT-3′) were synthesized by GenePharma (Shanghai, China).

ER Stress Reporter Assay

Transfections were performed using a Lipofectamine 2000 kit (Invitrogen) according to the manufacturer's instructions. Control cells and cells that were stably transfected with miR-122 (1-3 × 10^4 cells) were transfected with different reporter plasmids (100 ng per well) using the Cignal ERSE Reporter kit (SABiosciences, Frederick, MD). Twenty-four hours after transfection, the cells were treated with 1 μM thapsigargin (TG; Sigma) to modulate the UPR signaling pathway. The cells were harvested 24 hours after treatment and used to perform a dual luciferase assay. The luciferase assay was developed with the Dual-Luciferase Reporter Assay System (Promega, Madison, WI) according to the manufacturer's instructions.

Assessment of Caspase 3/7 Activity in Cells Stimulated by DOX

Caspase 3 activity was assessed using the ApoONE Homogeneous Caspase 3/7 Assay (Promega) according to the manufacturer's instructions. Cells were cultured in 96-well culture dishes to 50% to 70% confluence. To induce cell apoptosis, cells were treated with DOX (1 μg/ml). Caspase 3/7 activity was analyzed after a 24-hour incubation.

3′ Untranslated Region Constructs and Luciferase Assay

The 3′ untranslated region (UTR) of CDK4 containing an intact miR-122 recognition sequence was amplified by PCR using genomic DNA. The PCR product was subcloned into a pGL3 promoter vector (Promega) immediately downstream of the luciferase gene. The primers used were as follows: forward, 5′-CCCAAGCTTCATGTGGAGTGTTGGCTGTATC-3′; and reverse, 5′-GACTAGTGGAAAGGGACAAGAGGGAAC-3′. Cells were seeded into 24-well plates and cotransfected with 0.5 μg of the respective pmiR-3′UTR construct and 0.05 μg of the pRL-TK vector (Promega) using the Lipofectamine 2000 kit (Invitrogen). The pRL-TK vector was used as an internal control. After 48 hours, the luciferase activity was measured using the Dual-Luciferase Reporter Assay System (Promega).

Nude Mouse HCC Model

All of the mice used in this experiment received humane care. To image tumor chemosensitivity in mice, Huh7 cells were transfected with pCMV-Luciferase (Promega) and selected with neomycin (800 μg/ml). Five million of these cells were injected into the flanks of nude mice, and tumor cell activity was monitored using the IVIS Lumina II system (Caliper Life Sciences, Hopkinton, MA) 5 minutes after intraperitoneal injection of 4.0 mg of luciferin (Gold Biotech, St Louis, MO) in 50 μl of saline.

The pEZX-miR-122 HepG2 tumors were established by intradermally injecting 5 × 10^6 tumor cells in 80 μl of minimum essential medium into the back flanks of female nude mice (day 0). Tumor sizes were measured every 5 days using a slide caliper.

Terminal Deoxynucleotidyl Transferase-Mediated Deoxyuridine Triphosphate Nick-end Labeling Assay

The extent of hepatocyte apoptosis was detected using the terminal deoxynucleotidyl transferase-mediated deoxyuridine triphosphate nick-end labeling (TUNEL) assay. TUNEL-positive cells were counted using the random selection of high-power fields (400×) distributed over six independent sections. The numbers of TUNEL-positive and TUNEL-negative cells were compiled.

Statistical Analysis

The results are expressed as mean ± SD of the mean. The comparisons between the groups were performed using the Student's *t* test or the analysis of variance test as appropriate. The reported *P* values were two-sided and were considered significant when less than .05.

Results

Up-regulation of ER Stress Chaperone Proteins in Huh7 Cells That Are Transfected with the miR-122 Inhibitor

The novel proteomic methods allowed us to detect interaction mechanisms among a wider scope of targets [24,29]. In the current study, we transiently transfected Huh7 cells with the miR-122 inhibitor and control RNA. The suppressive effect of the miR-122 inhibitor was demonstrated using TaqMan real-time PCR, which showed that the expression level of miR-122 was decreased by 72% in the Huh7 cells that were transfected with the miR-122 inhibitor (Figure 1*A*).

Two-dimensional DIGE was used to observe differences in protein expression between miR-122 inhibitor–transfected and control RNA-transfected Huh7 cells. After DIGE, the Cy2, Cy3, and Cy5 channels of each gel were individually imaged for each gel, and the images were analyzed using DeCyder 5.0 software (GE Healthcare, Uppsala, Sweden). The intensity values of 2153 protein spots were measured (Figure 1*B*). To identify proteins that were differentially expressed between the miR-122 inhibitor–transfected Huh7 cells and control RNA–transfected Huh7 cells, we performed a Kruskal-Wallis test and applied the Bonferroni adjustment. We selected the protein spots that had a Bonferroni-adjusted $P <$ .01 and a greater than 1.3-fold change between the control- and

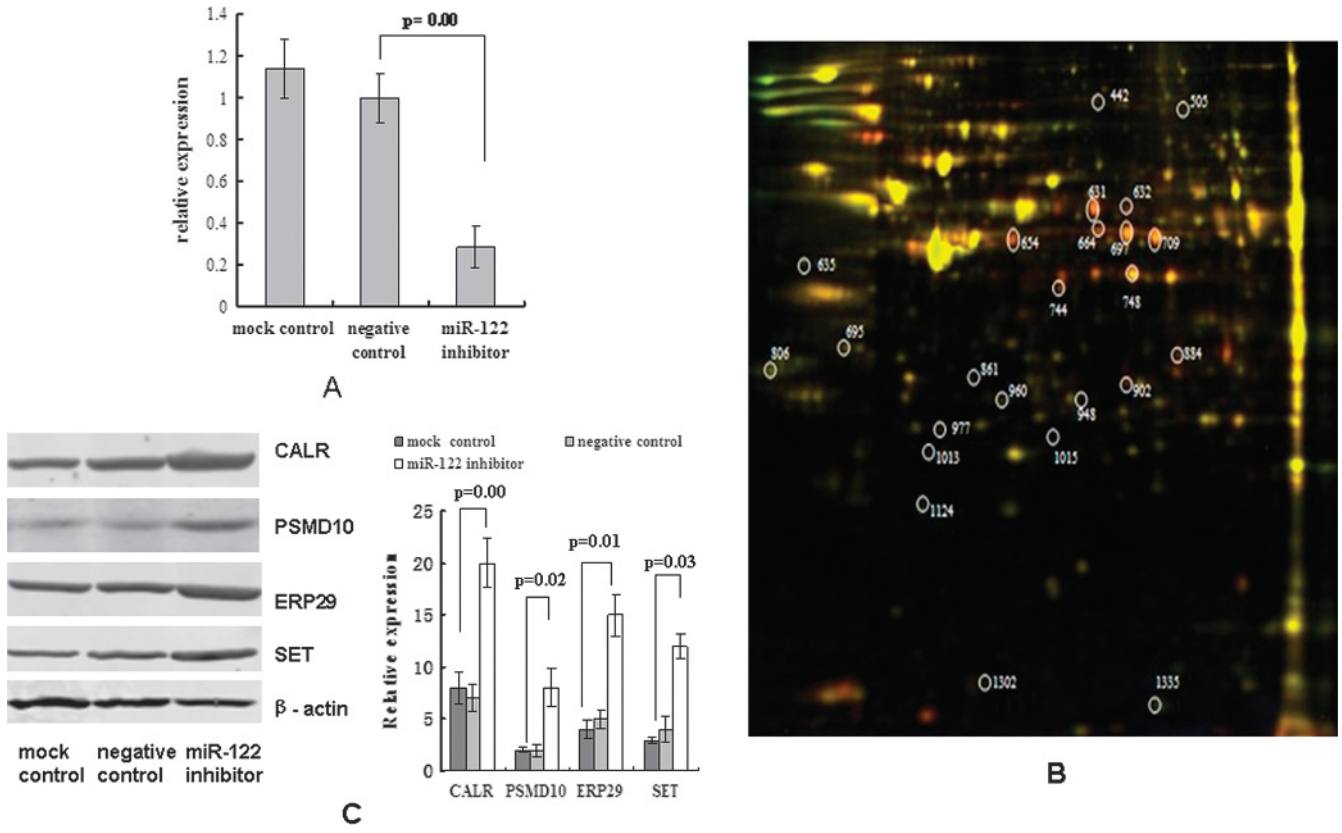

Figure 1. Down-regulation of miR-122 in Huh7 cells and the differentially expressed protein spots displayed in two-dimensional DIGE images. (A) Huh7 cells were transiently transfected with the miR-122 inhibitor or the control RNA. After 48 hours, the transfected cells were harvested for real-time PCR analysis of the miR-122 expression. Values indicate the 72% reduction of miR-122 expression in miR-122 inhibitor–transfected Huh7 cells compared to that in the control cells. (B) The extracted proteins were labeled with fluorescent dyes and separated using DIGE. The numbered spots indicate the differentially expressed protein spots. (C) CALR, SET, ERP29, and PMSD10 were overexpressed when the miR-122 was inhibited in Huh7 cells. Western blot analysis was used to assess the expression level of the four proteins. A representative blot (left) and the numeric data obtained from the densitometry analysis of the blots (right; $n = 4$) are shown.

miR-122 inhibitor–transfected cells. Thirty-three protein spots met these criteria. Mass spectrometry identified 19 unique proteins (Table W2) corresponding to the 33 protein spots. The functional classification according to Gene Ontology (www.geneontology.org) demonstrated that multiple identified proteins (4/19 proteins) were ER-localized or ER stress–associated proteins (Table W2). Other proteins were involved in DNA binding, protein binding, catalytic activity and structural molecule activity. The expression of the ER stress chaperones calreticulin (CALR), ER protein 29 (ERP29) and SET were increased when miR-122 was inhibited (Figure 1*C*). Interestingly, we also demonstrated that PSMD10, which enhanced the ER folding capacity and promoted recovery from ER stress through GRP78 [11], was overexpressed in miR-122 inhibitor–transfected Huh7 cells (Figure 1*C* and Table W2).

Ectopic Overexpression of miR-122 in HepG2 Cells and the Suppression of the UPR

To further examine the relationships among miR-122, UPR, and HCC, we generated a model of miR-122 up-regulation in HepG2 cells, which do not express miR-122 [26]. Stably expressing pEZX–miR-122 clones were identified using TaqMan real-time PCR (Figure 2*A*). The miR-122 expression level of clone 1 was increased 32-fold compared to that in HepG2 cells that were transfected with pEZX control plasmids. The HepG2–miR-122 clone 1 cells were used in subsequent experiments.

To investigate whether the expression of miR-122 affected the expression of other ER stress markers in the presence of the ER stress inducer TG, the expression of GRP78, p-eIF2α, and p-IRE1α was significantly decreased in HepG2–miR-122 cells (Figure 2*B*). In addition, the mRNA expression of GRP78 and CHOP was significantly decreased in HepG2–miR-122 cells compared to that in the HepG2–control cells at every time point after TG addition (Figure 2*C*). These results suggest that the ectopic expression of miR-122 negatively regulates the expression of important ER stress chaperones.

To further observe the effect of miR-122 on ER stress *in vitro*, the Cignal ERSE Reporter kit was used to monitor the ER stress response. The luciferase activity was decreased in miR-122 mimic–transfected HepG2 cells (Figure 2*D*, *left*) and in HepG2 cells that stably overexpressed miR-122 (Figure 2*D*, *right*). These results further demonstrate that miR-122 represses the UPR pathway.

miR-122 Inhibitor Enhances PSMD10 Stability through Its Target Gene CDK4

We selected PSMD10 for further study based on the several considerations. First, our proteomic results suggest that miR-122 may regulate the UPR pathway. In addition, a recent study reported that

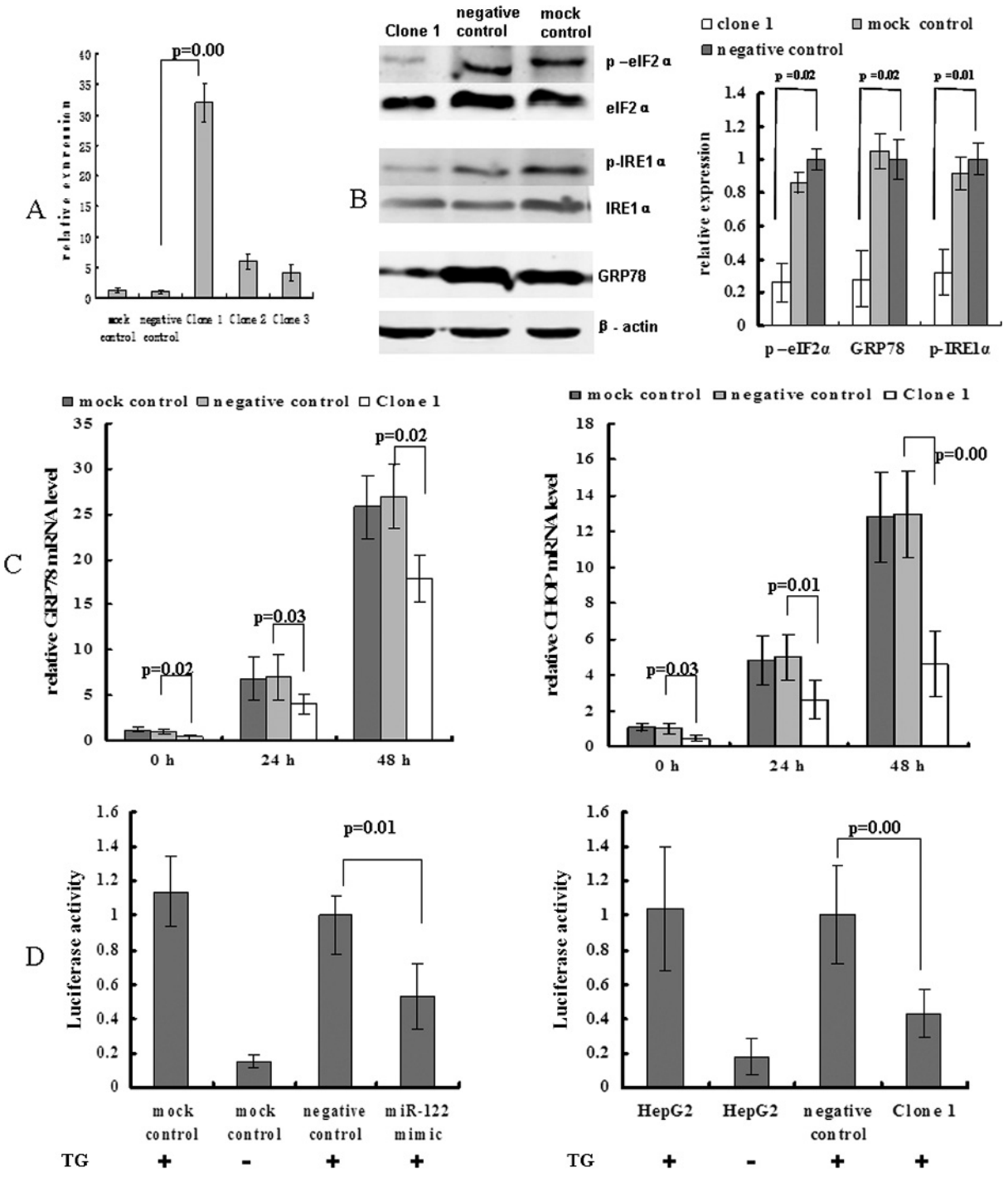

Figure 2. Screening of HepG2 cells that stably overexpressing miR-122 and the ER stress reporter assay. (A) The expression level of miR-122 was measured in stably transfected clones. Clone 1, which displayed a 32-fold increase in the miR-122 expression, had the highest miR-122 expression level. Clone 1 was used as a stable miR-122–overexpressing HepG2 cell line throughout the study. (B) Western blot analysis was used to assess the protein expression of GRP78, p-eIF2α, and p-IRE1α in HepG2–miR-122 cells (clone 1) compared to that in HepG2–control cells at 24 hours after TG addition. A representative blot (left), and the numeric data obtained from the densitometry analysis of the blots (right; $n = 4$) are shown. (C) The mRNA expression of GRP78 (left) and CHOP (right) was significantly decreased in HepG2–miR-122 cells (clone 1) compared to that in HepG2–control cells (negative control) at every time point after TG addition. (D) For the ER stress reporter assay, miR-122 mimic–transfected HepG2 cells (1-3 $\times$ 10^4 cells) were transfected with different reporter plasmids (100 ng per well) using the Cignal ERSE Reporter kit at 6 hours after mimic transfection. Other experiment procedures were performed as described in Materials and Methods. The luciferase activity was decreased in miR-122 mimic–transfected HepG2 cells (left) and clone 1 cells (right). All data represent the mean values $\pm$ SD from experiments performed at least five times.

PSMD10 enhanced the UPR and upregulated GRP78 expression [11]. Second, PSMD10 interacts with a predicted target gene of miR-122 called CDK4 [9]. Third, PSMD10 is consistently overexpressed in HCC, promotes tumor growth and inhibits apoptosis in HCC cells [9,10].

PSMD10 is an ankyrin-repeat oncoprotein that interacts with CDK4 [9], which is a miR-122–predicted target gene. We first validated whether CDK4 was a target gene of miR-122. The 3′UTR of CDK4 contains a putative miR-122 binding site (Figure 3*A*). To test whether the predicted binding sites in CDK4 mRNA could mediate repression of translation by miR-122, the 3′UTR of CDK4 was subcloned downstream of the luciferase gene in the pGL3 control vector. This construct was assayed in HEK293T cells transfected with a miR-122 mimic. As shown in Figure 3*B*, cells that were transfected with the reporter construct containing the 3′UTR of CDK4 had significantly lower luciferase activity after the cells cotransfected with the miR-122 mimic compared to cells that were cotransfected with control RNA. To confirm the results of the 3′UTR reporter assay, the expression of CDK4 was assessed in Huh7 cells that were transfected with the miR-122 inhibitor and in HepG2 cells that were transfected with miR-122 mimics using Western blot analysis. CDK4 was decreased in miR-122 mimic–transfected HepG2 cells (Figure 3*C*) or in stable miR-122–expressing HepG2 cells (Figure 3*D*) and increased in miR-122 inhibitor–transfected Huh7 cells (Figure 3*E*). Results of the Western blot assays

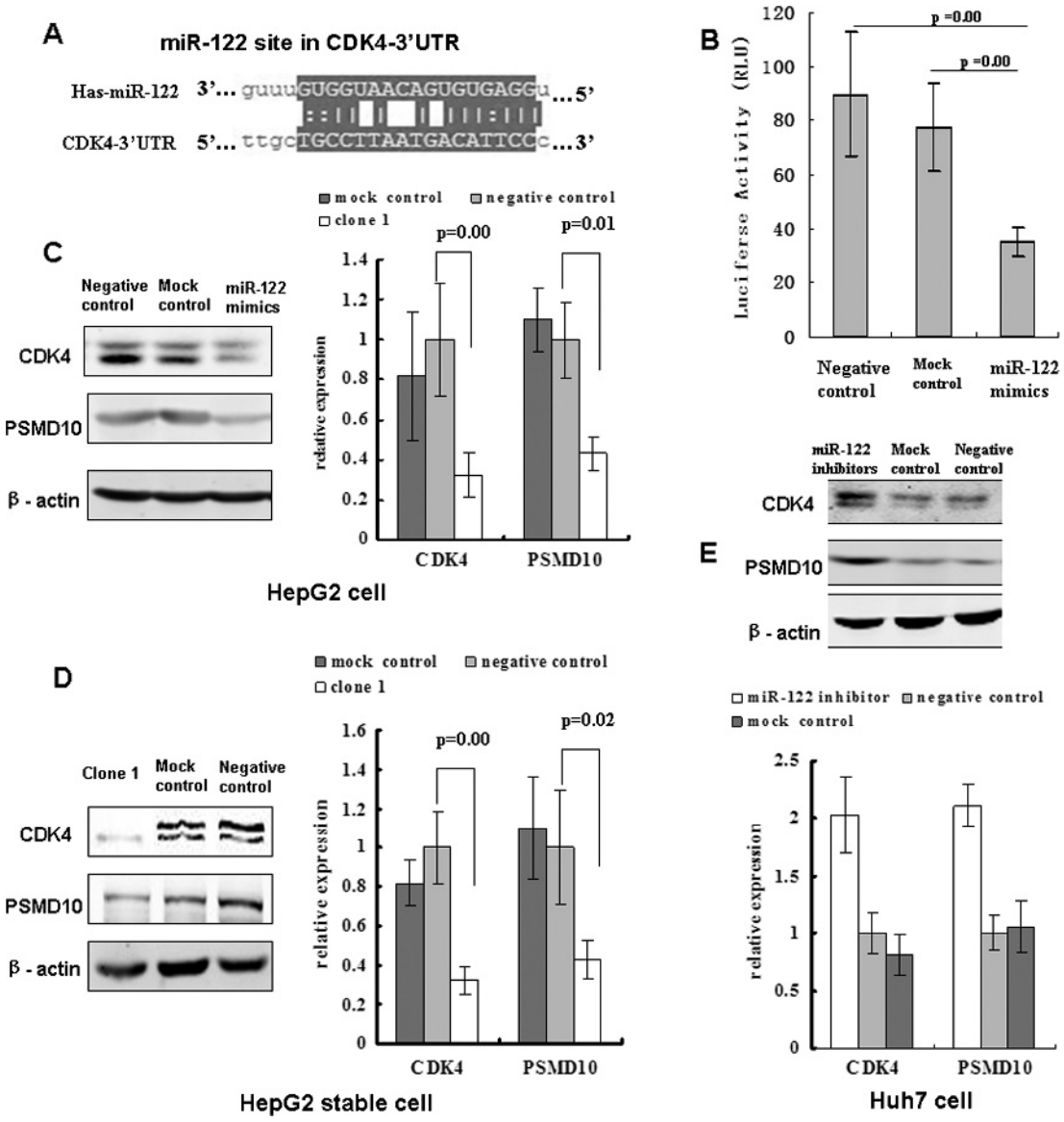

Figure 3. CDK4 was confirmed as a target of miR-122. (A) The miR-122 binding site in the 3′UTR of CDK4 is shown. (B) The verification of binding site specificity is shown. The reduction of the luciferase activity that was driven by the CDK4-3′UTR construct was observed in cells transfected with miR-122 mimic. (C, D, and E) The negative regulation of CDK4 by miR-122 was demonstrated using Western blot analysis. These results indicates that the protein expression of CDK4 is inhibited in miR-122 mimic–transfected HepG2 cells (C), stable miR-122–expressing HepG2 cells (D) and is increased in the miR-122 inhibitor–transfected Huh7 cells (E). The expression of PSMD10 was also changed based on the level of miR-122. The representative blots (left) and numeric data obtained from densitometry analysis of the blots (right, $n = 4$) are shown.

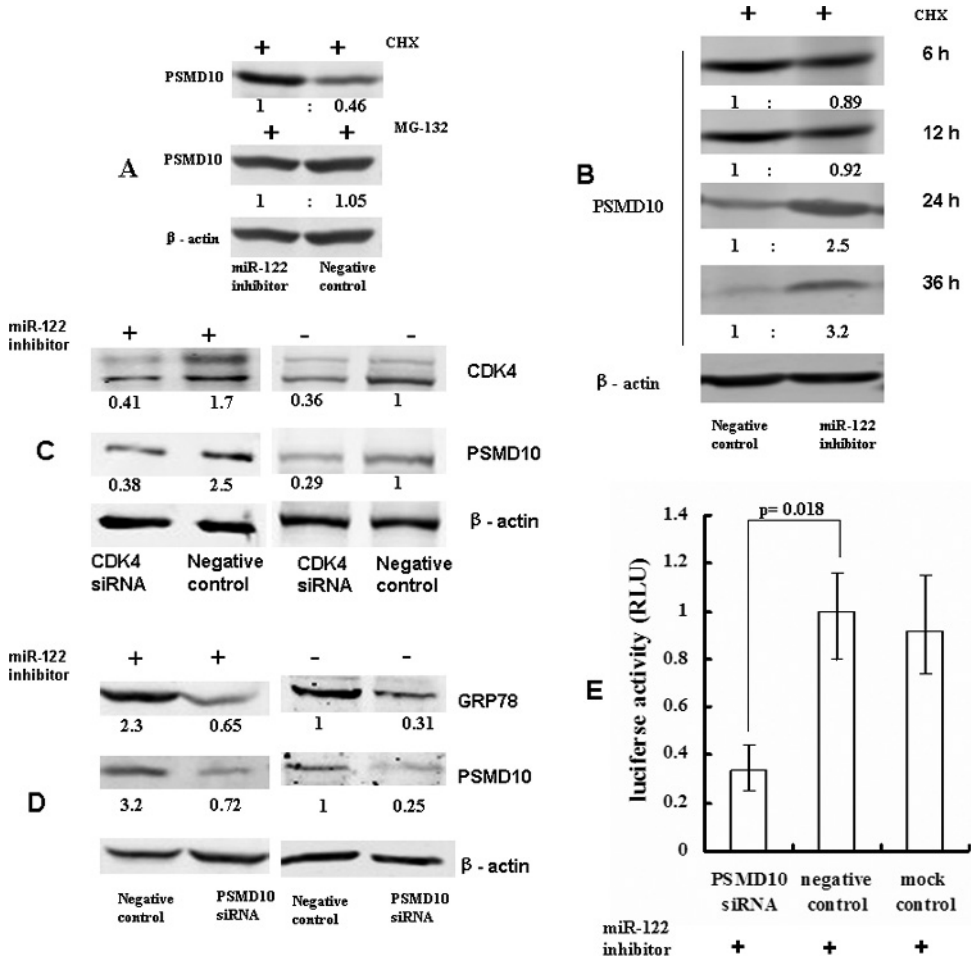

Figure 4. The miR-122 inhibitor enhanced the PSMD10 stability through its target gene *CDK4*. (A) At 24 hours after the miR-122 inhibitor and the negative control were transfected, Huh7 cells were incubated with the protein synthesis inhibitor cycloheximide (CHX, 0.5 μg/μl) or the proteasome inhibitor MG-132 (5 μM) for another 24 hours. The protein expression of PSMD10 was detected using Western blot analysis. MG-132 treatment but not CHX treatment abolished the change in the expression of PSMD10 in miR-122 inhibitor– and negative control-transfected cells. (B) At 6 hours after the miR-122 inhibitor and the negative control were transfected, Huh7 cells were incubated with CHX (0.5 μg/μl) for another 6, 12, 24, or 36 hours. The protein expression of PSMD10 was detected using Western blot analysis. (C) siRNA against CDK4 abolished the increased PSMD10 protein expression in miR-122 inhibitor–transfected Huh7 cells (n = 4). (D) PSMD10 siRNA decreased GRP78 protein expression in miR-122 inhibitor–transfected Huh7 cells (n = 4). (E) The miR-122 inhibitor and PSMD10 siRNA–cotransfected Huh7 cells were treated as described in Figure 2*D*. The results from the ER stress reporter assay show that the luciferase activity is decreased in miR-122 inhibitor–transfected Huh7 cells transfected with PSMD10 siRNA (n = 4). For Western blot analysis, the relative ratios after normalization are shown below each panel.

confirmed the 3′UTR reporter assay results. Furthermore, the changes in the expression of PSMD10 correlated to the changes in the expression of CDK4.

We did not detect up-regulation of PSMD10 transcription after miR-122 was inhibited in Huh7 cells (data not shown). To detect whether the miR-122 inhibitor enhanced PSMD10 stability, we treated miR-122–repressed Huh7 cells with the protein synthesis inhibitor cycloheximide (CHX) or the proteasome inhibitor MG-132. As shown in Figure 4*A*, only MG-132 abolished the up-regulation of PSMD10 protein levels in miR-122 inhibitor–treated Huh7 cells. A time course detection of PSMD10 degradation after CHX addition was performed to determine whether there was more initial total PSMD10 protein or whether PSMD10 degraded more slowly. As shown in Figure 4*B*, the protein level of PSMD10 between the miR-122 inhibitor– and negative control-transfected Huh7 cells was different at 24 hours after CHX addition. This difference could also be detected at 36 hours but not 6 or 12 hours after CHX addition. This finding indicates that the miR-122 inhibitor enhances PSMD10 stability.

We supposed that miR-122 might enhance PSMD10 stability through CDK4. We performed a Western blot analysis to examine the protein level of PSMD10 in miR-122–repressed Huh7 cells that were treated with siRNAs against CDK4. As shown in Figure 4*C*, PSMD10 protein levels were decreased after the treatment with CDK4 siRNAs. These results indicate that the up-regulation of the miR-122 target gene CDK4 is essential for PSMD10 accumulation in miR-122 inhibitor–treated Huh7 cells.

miR-122 Negatively Regulates the UPR through the CDK4-PSMD10 Chaperone Pathway

A recent study reported that PSMD10 enhanced the UPR and up-regulated GRP78 expression [11]. Therefore, we further investigated whether PSMD10 was involved in the miR-122–mediated negative

regulation of the UPR. We used a Cignal ERSE Reporter kit to monitor the activity of the ER stress response in miR-122 inhibitor–treated Huh7 cells that were also knocked down for PSMD10 expression. The luciferase activity was decreased in cells that were also knocked down for PSMD10 expression (Figure 4*D*). GRP78 expression was also dramatically reduced in miR-122 inhibitor–treated Huh7 cells when PSMD10 expression was knocked down (Figure 4*E*). Based on these findings, we concluded that the miR-122 inhibitor increased the UPR at least partly by upregulating PSMD10.

PSMD10 Is Associated with the Proapoptotic Role of miR-122 In Vitro *and* In Vivo

Considering that the UPR is an adaptive response that increases cell survival under stress conditions, we further explored whether the CDK4-PSMD10-UPR pathway played a key role in drug resistance. We treated miR-122–repressed Huh7 cells with cisplatin or DOX and measured the cell survival using a CCK-8 kit and the chemotherapeutic agent–triggered apoptosis using a caspase 3 activity assay. Cells that were transfected with the miR-122 inhibitor displayed lower levels of apoptosis in response to cisplatin (Figure 5, *A* and *B*). This result was confirmed using a gain-of-function analysis, which showed that miR-122 enhanced the sensitivity of HepG2 cells to cisplatin or DOX (data not shown). We next investigated whether siRNAs against PSMD10 could enhance the chemosensitivity of Huh7 cells that were transfected with the miR-122 inhibitor. In the miR-122 inhibitor–transfected Huh7 cells, reduced expression of PSMD10 resulted in a significant increase in DOX-triggered apoptosis (Figure 5, *C* and *D*). Taken together, the results of gain- and loss-of-function studies imply that the miR-122 inhibitor may reduce the sensitivity of HCC cells to chemotherapeutic agent–induced apoptosis and that PSMD10 may play an important role in this process.

To further confirm the *in vitro* experiment results, we generated a human miR-122 inhibitor expression plasmid (miRZip–miR-122) and an RNAi expression vector for human PSMD10 (shRNA-PSMD10). We next evaluated the effect of the miR-122–PSMD10 pathway on chemosensitivity of Huh7 cells using an *in vivo* model. Stable cell lines expressing firefly luciferase were injected into the flanks of nude mice (four mice for each treatment group). After the tumors were established (day 0), each plasmid (100 μg of a plasmid in 80 μl of PBS) was injected intratumorally on days 0 and 2. On days 3 and 6, 6 mg/kg of DOX was intravenously injected through the tail vein. On days 6, 9, and 12, the mice were imaged. The effectiveness of miRZip–miR-122 and

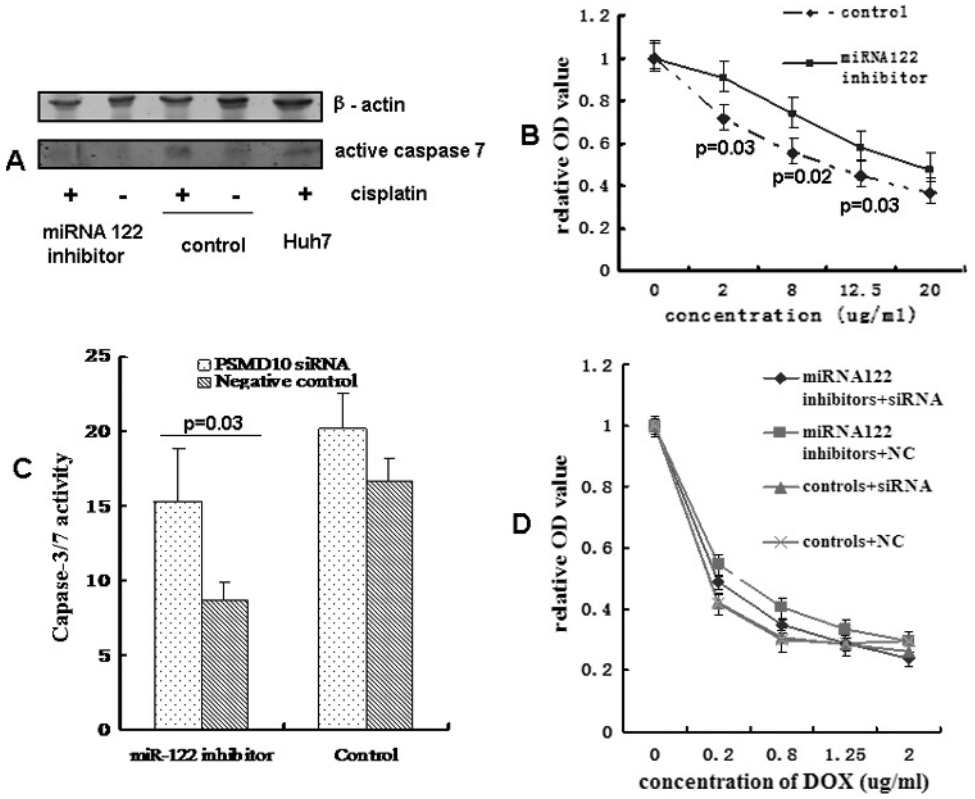

Figure 5. PSMD10 mediated miR-122 inhibitor–induced drug resistance. (A) Western blot detection of cleaved caspase 3 is shown. Twenty-four hours after Huh7 cells were transfected with the miR-122 inhibitor or the control, Huh7 cells were incubated with cisplatin (8 μg/ml) for another 24 hours. C-Caspase3 indicates cleaved caspase 3 ($n = 4$). (B) The relative live cell number was determined using the CCK-8 assay (mean ± SD). Huh7 cells were incubated with different concentrations of cisplatin for another 24 hours after transfection with the miR-122 inhibitor or the control ($n = 4$). (C) Caspase 3/7 activity was detected using an ApoONE Homogeneous Caspase 3/7 Assay. Twenty-four hours after Huh7 cells were cotransfected with the miR-122 inhibitor and siRNA against PSMD10 or respective control, Huh7 cells were stimulated with DOX (1 μg/ml) for another 24 hours. (D) Relative live cell number was determined by way of CCK-8 assay. Twenty-four hours after Huh7 cells were transfected with the miR-122 inhibitor, siRNA against PSMD10 or their respective controls. Huh7 cells were stimulated with different concentrations of DOX for another 24 hours. siRNA, siRNA against PSMD10; Control indicates the corresponding negative control for miR-122 inhibitor; NC, the corresponding negative control for siRNA against PSMD10. (For 0.2 μg/ml, miR-122 inhibitor + NC *vs* controls + NC [$P = .032$], miR-122 inhibitor + siRNA *vs* controls + NC [$P = .56$]; for 0.8 μg/ml, miR-122 inhibitor + NC *vs* controls + NC [$P = .028$], miR-122 inhibitor + siRNA *vs* controls + NC [$P = .82$]; $n = 4$).

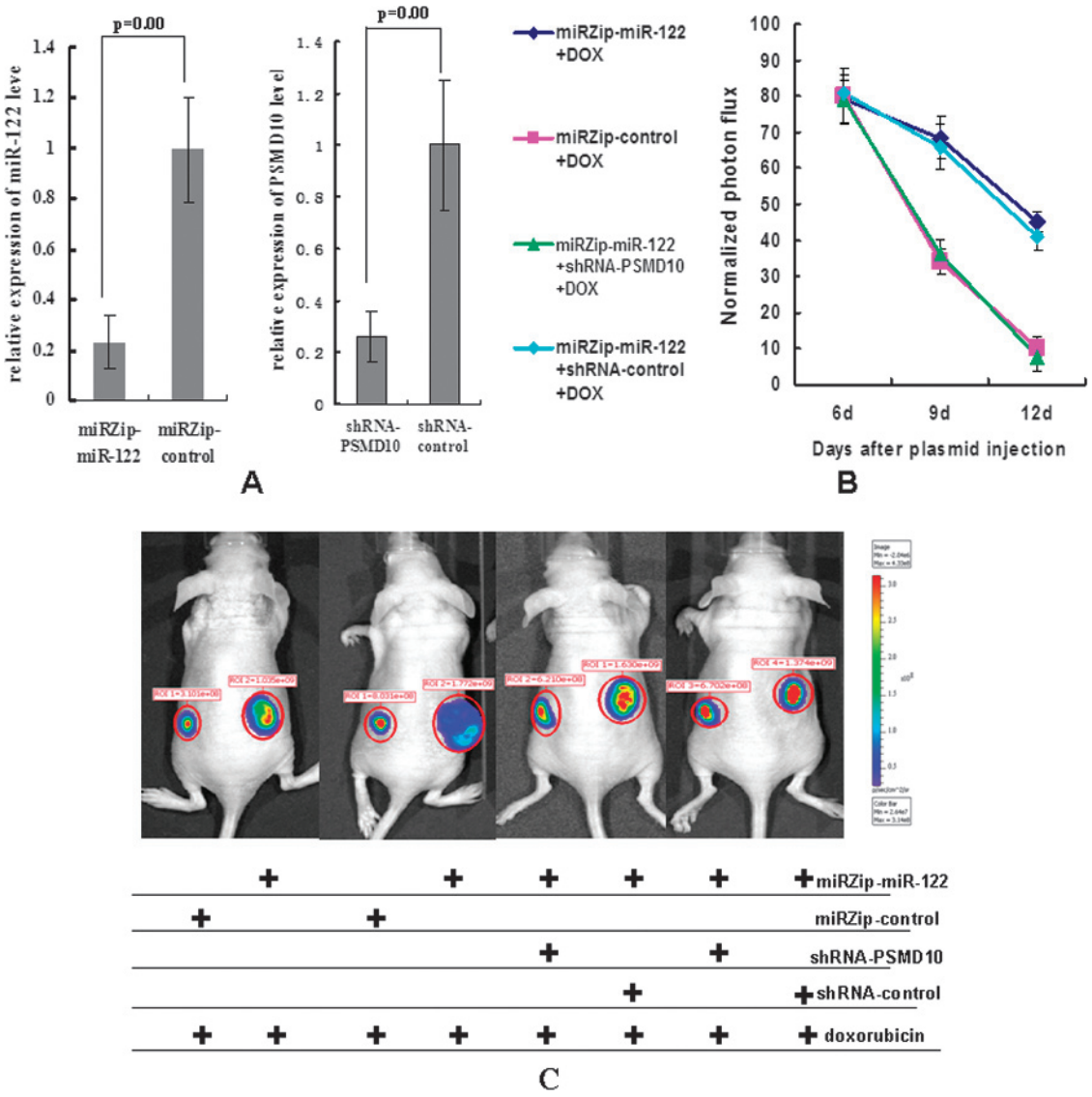

Figure 6. Tumor chemotherapy in nude mice. Tumor establishment, plasmids, and DOX injection were performed as described in the main text. (A) The effectiveness of the plasmids miRZip–miR-122 and shRNA-PSMD10 was examined by real-time PCR using tumor tissues implanted in nude mice. (B) The relative luciferase signal captured in each tumor at different time points is shown ($n = 4$). On days 6, 9, and 12 after the intratumorally injection of plasmid, the mice were imaged using IVIS Lumina II System as described in Materials and Methods. (C) Photographs of tumors that developed in mice were obtained by imaging with the IVIS system. The representative of luciferase signal (ROI) was captured in each group at day 9 after the plasmid injection. The most effective RNAi expression vector for human PSMD10, shRNA-PSMD10, was used.

shRNA-PSMD10 were examined by real-time PCR using the tumor tissues that were implanted in nude mice. As shown in Figure 6*A*, miRZip–miR-122 and shRNA-PSMD10 had an effect on their respective targets after being injected into nude mice. The quantification of the luciferase signal showed that PSMD10 shRNA (shRNA-PSMD10 plasmid) abolished the miR-122 inhibitor–induced drug resistance *in vivo* (Figure 6*B*). Representative photographs of tumors in nude mice are shown in Figure 6*C*.

Discussion

MicroRNAs are posttranscriptional modulators of gene expression and play an important role in many developmental and metabolic processes [12]. Many studies have shown that miR-122 inhibited many characteristic properties of cancer cells, including clonogenic survival, anchorage-independent growth, migration, invasion, epithelial-mesenchymal transition, and tumorigenesis in nude mice [22]. More recently, a study revealed that miR-122 regulated mitochondrial metabolism and that its loss might contribute to the morbidity and mortality of liver cancer [30]. Although many identified targets of miR-122 are involved in differentiation, cell cycle progression, invasion, metastasis, and tumorigenesis, the relationships between the different functions and miR-122 targets remain to be elucidated in a broader perspective. More importantly, some studies have found that miRNA secondary targets and downstream pathways may form a more sensitive measure of miRNA function than the direct measurements of miRNA expression levels or miRNA target genes [30,31]. Proteomics, which was an approach that can simultaneously analyze multiple proteins changes, is used to scan the miRNA secondary targets and downstream pathways.

Recently, many new proteomic approaches have been applied to miRNA research [24,25,29,32]. In the current study, we inhibited the expression of miR-122 in Huh7 cells and identified differentially expressed proteins using DIGE. Our results show that four of these proteins are known UPR-related proteins (Table W1 and Figure 1, *B* and *C*). CALR is an ER chaperone that acts in the proper folding of many proteins and glycoproteins through the calreticulin/calnexin cycle [33]. ERP29 is widely thought to be a folding assistant for secretory proteins and probably functions as a protein disulfide isomerase-like molecular chaperone [34]. Some studies have shown that SET-mediated dephosphorylation of BCL-2 is required to protect BCL-2 from proteasome-dependent degradation, which affects the resistance to ER stress [35], PSMD10, which is consistently overexpressed in HCC, has been shown to promote tumor growth and inhibit apoptosis in HCC cells by enhancing the UPR and upregulating GRP78 expression [11]. Therefore, we speculated that miR-122 affected hepatocarcinogenesis and apoptosis through UPR.

For further confirmation of the effect of miR-122 on ER chaperones and UPR, we screened stable HepG2 cell clones that overexpressed miR-122 (Figure 2*A*). Results from the assays using the ERSE reporter, which contains binding sites for the transcription factors NF-Y/CBF and YY1, show that miR-122 overexpression decreases the activity of the UPR pathway (Figure 2, *C* and *D*). More importantly, our results demonstrate that expressions of important ER stress chaperones, GRP78 and CHOP, are repressed by the overexpression of miR-122 after TG stimulation. GRP78, which is a member of the highly conserved Hsp70 protein family, is constitutively expressed and is upregulated on UPR activation [36]. Increased expression of GRP78 enhances the protein folding capacity of the ER and is associated with prosurvival responses [37]. The repression of the UPR by miR-122 may decrease the protein folding capacity of the ER and plays a proapoptotic role in carcinoma cells. Given that phosphorylated eIF2α inhibits translation initiation thus promoting global attenuation of protein translation, this study suggests that miRNA-122 has a dual role in translational control. This inference is in accordance with previous reports that described how miR-122 acted as a tumor suppressor gene for hepatocarcinogenesis [19,20,22].

PSMD10 contains six ankyrin repeats and interacts with CDK4 and the S6 ATPase of the 26S proteasome [9]. To elucidate the mechanism by which miR-122 negative regulated the UPR pathway, we predicted the target genes of miR-122 and identified these target genes using a 3′ UTR reporter assay (Figure 3, *A* and *B*). The regulation of CDK4 expression by miR-122 was validated in miR-122 mimic transfected HepG2 cells (Figure 3*C*), stable miR-122–expressing HepG2 cells (Figure 3*D*), and miR-122 inhibitor–transfected Huh7 cells (Figure 3*E*). Interestingly, our results indicate that the up-regulation of the miR-122 target gene *CDK4* is essential for the PSMD10 accumulation in miR-122 inhibitor–treated Huh7 cells (Figure 4*C*). A recent study provided evidence that PSMD10 protected HCC cells from ER stress–induced apoptosis through the enhancement of UPR signaling [11]. Therefore, we hypothesized that PSMD10 was a key link between miR-122 and UPR signaling. Indeed, our results indicate that PSMD10 is at least partly responsible for the increased expression of GRP78 and UPR signaling on inhibition of miR-122 (Figure 4, *D* and *E*).

With respect to cancer, many aspects of the UPR pathway are cytoprotective and help cancer cells to withstand the stress that is caused by hypoxia, nutrient deprivation, or anticancer treatment. Activation of the UPR pathway might promote dormancy, aid tumor growth, or alter tumor chemosensitivity. In the current study, we found that down-regulation of miR-122 in Huh7 cells increased the expression of PSMD10 and subsequently enhanced UPR signaling. The effect of the miR-122–PSMD10-UPR pathway on antitumor drug–associated apoptosis was also examined *in vitro* and *in vivo*. In summary, this pathway plays key roles in drug resistance (Figures 5 and 6). First, miR-122 inhibitor enhanced the drug tolerance of p53 mutant Huh7 cells (Figure 5, *A* and *B*). More importantly, siRNAs against PSMD10 increased anticancer drug–mediated apoptosis in miR-122–repressed Huh7 cells (Figures 5, *C* and *D*, and 6). A previous study demonstrated that the miR-122/cyclin G_1 interaction affected the DOX sensitivity of HCC cells by mediating p53 activity [23]. Furthermore, the same study showed that miR-122 also influenced the sensitivity of HCC cells to DOX through a p53-independent apoptosis pathway [23]; however, the mechanism by which this phenomenon occurred is unknown. Therefore, our findings expand on these results: we may have identified the miR-122–PSMD10-UPR pathway as the p53-independent apoptosis pathway observed in the previous study [23].

When injected into nude mice, tumor cells can grow under stressed microenvironments such as those caused by ischemia, hypoxemia, or nutrient deprivation. Tumor growth was inhibited in our miR-122–overexpressing HepG2 cells, and the percentage of cells undergoing apoptosis was increased in miR-122–overexpressing tumors compared to that in control tumors (Figure W1). Understanding the relationships among miR-122, UPR, and apoptosis will be helpful to reveal the molecular mechanisms involved in hepatocarcinogenesis and to identify novel therapeutic targets.

In summary, we have clearly demonstrated that miR-122 negatively regulates UPR chaperones and we have identified a miR-122–PSMD10-UPR pathway, both of which support the potential application of miR-122 in HCC chemotherapy.

References

[1] Kim I, Xu W, and Reed JC (2008). Cell death and endoplasmic reticulum stress: disease relevance and therapeutic opportunities. *Nat Rev Drug Discov* **7**, 1013–1030.

[2] Onn A and Ron D (2010). Modeling the endoplasmic reticulum unfolded protein response. *Nat Struct Mol Biol* **17**, 924–925.

[3] Healy SJ, Gorman AM, Mousavi-Shafaei P, Gupta S, and Samali A (2009). Targeting the endoplasmic reticulum–stress response as an anticancer strategy. *Eur J Pharmacol* **625**, 234–246.

[4] Ma Y and Hendershot LM (2004). The role of the unfolded protein response in tumour development: friend or foe? *Nat Rev Cancer* **4**, 966–977.

[5] Scriven P, Brown NJ, Pockley AG, and Wyld L (2007). The unfolded protein response and cancer: a brighter future unfolding? *J Mol Med* **85**, 331–341.

[6] Luk JM, Lam CT, Siu AF, Lam BY, Ng IO, Hu MY, Che CM, and Fan ST (2006). Proteomic profiling of hepatocellular carcinoma in Chinese cohort reveals heat-shock proteins (Hsp27, Hsp70, GRP78) up-regulation and their associated prognostic values. *Proteomics* **6**, 1049–1057.

[7] Shuda M, Kondoh N, Imazeki N, Tanaka K, Okada T, Mori K, Hada A, Arai M, Wakatsuki T, Matsubara O, et al. (2003). Activation of the *ATF6*, *XBP1* and *grp78* genes in human hepatocellular carcinoma: a possible involvement of the ER stress pathway in hepatocarcinogenesis. *J Hepatol* **38**, 605–614.

[8] Al-Rawashdeh FY, Scriven P, Cameron IC, Vergani PV, and Wyld L (2010). Unfolded protein response activation contributes to chemoresistance in hepatocellular carcinoma. *Eur J Gastroenterol Hepatol* **22**, 1099–1105.

[9] Higashitsuji H, Itoh K, Nagao T, Dawson S, Nonoguchi K, Kido T, Mayer RJ, Arii S, and Fujita J (2000). Reduced stability of retinoblastoma protein by gankyrin, an oncogenic ankyrin-repeat protein overexpressed in hepatomas. *Nat Med* **6**, 96–99.

[10] Li H, Fu X, Chen Y, Hong Y, Tan Y, Cao H, Wu M, and Wang H (2005). Use of adenovirus-delivered siRNA to target oncoprotein p28GANK in hepatocellular carcinoma. *Gastroenterology* **128**, 2029–2041.

[11] Dai RY, Chen Y, Fu J, Dong LW, Ren YB, Yang GZ, Qian YW, Cao J, Tang SH, Yang SL, et al. (2009). p28GANK inhibits endoplasmic reticulum stress–induced

cell death via enhancement of the endoplasmic reticulum adaptive capacity. *Cell Res* **19**, 1243–1257.

[12] Lim LP, Glasner ME, Yekta S, Burge CB, and Bartel DP (2003). Vertebrate microRNA genes. *Science* **299**, 1540.

[13] Davidson-Moncada J, Papavasiliou FN, and Tam W (2010). MicroRNAs of the immune system: roles in inflammation and cancer. *Ann N Y Acad Sci* **1183**, 183–194.

[14] Shenouda SK and Alahari SK (2009). MicroRNA function in cancer: oncogene or a tumor suppressor? *Cancer Metastasis Rev* **28**, 369–378.

[15] Lagos-Quintana M, Rauhut R, Yalcin A, Meyer J, Lendeckel W, and Tuschl T (2002). Identification of tissue-specific microRNAs from mouse. *Curr Biol* **12**, 735–739.

[16] Xu H, He JH, Xiao ZD, Zhang QQ, Chen YQ, Zhou H, and Qu LH (2010). Liver-enriched transcription factors regulate microRNA-122 that targets CUTL1 during liver development. *Hepatology* **52**, 1431–1442.

[17] Girard M, Jacquemin E, Munnich A, Lyonnet S, and Henrion-Caude A (2008). miR-122, a paradigm for the role of microRNAs in the liver. *J Hepatol* **48**, 648–656.

[18] Kutay H, Bai S, Datta J, Motiwala T, Pogribny I, Frankel W, Jacob ST, and Ghoshal K (2006). Downregulation of miR-122 in the rodent and human hepatocellular carcinomas. *J Cell Biochem* **99**, 671–678.

[19] Tsai WC, Hsu PW, Lai TC, Chau GY, Lin CW, Chen CM, Lin CD, Liao YL, Wang JL, Chau YP, et al. (2009). MicroRNA-122, a tumor suppressor microRNA that regulates intrahepatic metastasis of hepatocellular carcinoma. *Hepatology* **49**, 1571–1582.

[20] Coulouarn C, Factor VM, Andersen JB, Durkin ME, and Thorgeirsson SS (2009). Loss of miR-122 expression in liver cancer correlates with suppression of the hepatic phenotype and gain of metastatic properties. *Oncogene* **28**, 3526–3536.

[21] Zeng C, Wang R, Li D, Lin XJ, Wei QK, Yuan Y, Wang Q, Chen W, and Zhuang SM (2010). A novel GSK-3 β-C/EBP α-miR-122–insulin-like growth factor 1 receptor regulatory circuitry in human hepatocellular carcinoma. *Hepatology* **52**, 1702–1712.

[22] Bai S, Nasser MW, Wang B, Hsu SH, Datta J, Kutay H, Yadav A, Nuovo G, Kumar P, and Ghoshal K (2009). MicroRNA-122 inhibits tumorigenic properties of hepatocellular carcinoma cells and sensitizes these cells to sorafenib. *J Biol Chem* **284**, 32015–32027.

[23] Fornari F, Gramantieri L, Giovannini C, Veronese A, Ferracin M, Sabbioni S, Calin GA, Grazi GL, Croce CM, Tavolari S, et al. (2009). miR-122/cyclin G_1 interaction modulates p53 activity and affects doxorubicin sensitivity of human hepatocarcinoma cells. *Cancer Res* **69**, 5761–5767.

[24] Baek D, Villen J, Shin C, Camargo FD, Gygi SP, and Bartel DP (2008). The impact of microRNAs on protein output. *Nature* **455**, 64–71.

[25] Yang F, Yin Y, Wang F, Wang Y, Zhang L, Tang Y, and Sun S (2010). miR-17-5p promotes migration of human hepatocellular carcinoma cells through the p38 mitogen-activated protein kinase–heat shock protein 27 pathway. *Hepatology* **51**, 1614–1623.

[26] Bhattacharyya SN, Habermacher R, Martine U, Closs EI, and Filipowicz W (2006). Relief of microRNA-mediated translational repression in human cells subjected to stress. *Cell* **125**, 1111–1124.

[27] Moenner M, Pluquet O, Bouchecareilh M, and Chevet E (2007). Integrated endoplasmic reticulum stress responses in cancer. *Cancer Res* **67**, 10631–10634.

[28] Yang F, Yin Y, Wang F, Zhang L, Wang Y, and Sun S (2010). An altered pattern of liver apolipoprotein A-I isoforms is implicated in male chronic hepatitis B progression. *J Proteome Res* **9**, 134–143.

[29] Selbach M, Schwanhausser B, Thierfelder N, Fang Z, Khanin R, and Rajewsky N (2008). Widespread changes in protein synthesis induced by microRNAs. *Nature* **455**, 58–63.

[30] Burchard J, Zhang C, Liu AM, Poon RT, Lee NP, Wong KF, Sham PC, Lam BY, Ferguson MD, Tokiwa G, et al. (2010). microRNA-122 as a regulator of mitochondrial metabolic gene network in hepatocellular carcinoma. *Mol Syst Biol* **6**, 402.

[31] Davis S, Propp S, Freier SM, Jones LE, Serra MJ, Kinberger G, Bhat B, Swayze EE, Bennett CF, and Esau C (2009). Potent inhibition of microRNA *in vivo* without degradation. *Nucleic Acids Res* **37**, 70–77.

[32] Grosshans H and Filipowicz W (2008). Proteomics joins the search for microRNA targets. *Cell* **134**, 560–562.

[33] Williams DB (2006). Beyond lectins: the calnexin/calreticulin chaperone system of the endoplasmic reticulum. *J Cell Sci* **119**, 615–623.

[34] Hubbard MJ, Mangum JE, and McHugh NJ (2004). Purification and biochemical characterization of native ERp29 from rat liver. *Biochem J* **383**, 589–597.

[35] Lin SS, Bassik MC, Suh H, Nishino M, Arroyo JD, Hahn WC, Korsmeyer SJ, and Roberts TM (2006). PP2A regulates BCL-2 phosphorylation and proteasome-mediated degradation at the endoplasmic reticulum. *J Biol Chem* **281**, 23003–23012.

[36] Kim R, Emi M, Tanabe K, and Murakami S (2006). Role of the unfolded protein response in cell death. *Apoptosis* **11**, 5–13.

[37] Reddy RK, Mao C, Baumeister P, Austin RC, Kaufman RJ, and Lee AS (2003). Endoplasmic reticulum chaperone protein GRP78 protects cells from apoptosis induced by topoisomerase inhibitors: role of ATP binding site in suppression of caspase-7 activation. *J Biol Chem* **278**, 20915–20924.

Supplementary Materials

Results

Studies have shown that overexpression of miR-122 suppresses *in situ* tumor formation. To study the role of miR-122 in tumor formation in our model, nude mice were injected with HepG2–miR-122 or HepG2–control cells. The tumor volume in mice that were injected with HepG2–miR-122 cells was smaller than that in mice that were injected with the HepG2–control cells (Figure W1, *A* and *B*). We further examined apoptosis in mice that were injected with each tumor type. The TUNEL results show that the frequency of apoptotic cells is significantly increased in HepG2–miR-122 tumors (Figure W1, *C* and *D*).

Table W1. Real-time PCR Primers.

Gene	Sequence	Product Size (bp)
GRP78	5′CCGTCCTATGTCGCCTTCACT3′ 5′TGTCTTTGTTTGCCCACCTCC3′	231
CHOP	5′CCACTCTTGACCCTGCTTCTC3′ 5′TGACCACTCTGTTTCCGTTTC3′	172
PSMD10	5′GGGGCTAATCCAGATGCTA3′ 5′ACTTGCTCCTTGGGACACC3′	207
GAPDH	5′ CGGATTTGGTCGTATTGGG 3′ 5′ CTGGAAGATGGTGATGGGATT 3′	208

Table W2. Differential Expression Proteins between miR-122 Inhibitors and Controls Transfected Huh7 Cells Identified by MALDI-TOF MS.

Master Spot ID*	Fold Change†	Accession No.‡	Name and Official Symbol	Coverage and Protein Score§	Molecular Function	Subcellular Location
635	2.2	gi|62897681	Calreticulin, CALR	26%/176	Ca(2+) binding, regulation of gene transcription	**Endoplasmic reticulum lumen**
505	2.01	gi|15149465	Caldesmon 1, CALD1	25%/263	Ca(2+) binding	Thin filaments Stress fibers
695	1.96	gi|4502551	Calumenin, CALU	55%/516	Protein folding and sorting	**Endoplasmic reticulum lumen**
948	1.95	gi|5803013	ER protein 29, ERP29	29%/90	Processing of secretory proteins within the ER	**Endoplasmic reticulum lumen**
806	1.86	gi|55663125	SET nuclear oncogene, SET	18%/167	Multitasking protein, involved in apoptosis, transcription, nucleosome assembly, and histone binding	Cytoplasm **Endoplasmic reticulum** Nucleus
960	1.69	gi|46249388	Phosphoserine phosphatase, PSPH	32%/129	Catalyzes the last step in the biosynthesis of serine from carbohydrates	—
977	1.63	gi|23065552	Glutathione *S*-transferase mu 3 (brain), GSTM3	46%/216	Conjugation of reduced glutathione to a wide number of exogenous and endogenous hydrophobic electrophiles	Cytoplasm
1015	1.62	gi|4506217	Proteasome (prosome, macropain) 26S subunit, non-ATPase, 10 PSMD10	23%/276	Acts as a regulatory subunit of the 26S proteasome which is involved in the ATP-dependent degradation of ubiquitinated proteins	Proteasome
861	1.59	gi|16198390	glyoxalase domain containing 4, GLOD4	30%/148	Inhibit the HCC cell growth	Mitochondrion
748	0.80	gi|1000094	Centromere protein F, 350/400ka (mitosin), CENPF	14%/73	Required for kinetochore function and chromosome segregation in mitosis	Cytoplasm, perinuclear region
1013	−0.69	gi|4885417	Ubiquitin-conjugating enzyme E2K (UBC1 homolog, yeast), UBE2K	40%/219	Catalyzes the covalent attachment of ubiquitin to other proteins	Cytoplasm
654	−0.53	gi|30311	Keratin 18, KRT18	26%/78	Involved in the uptake of thrombin-antithrombin complexes by hepatic cells	Cytoplasm, perinuclear region
632	−0.7	gi|307086	Keratin 10, KRT10	21%/118	Cytokeratin	—
631	−0.69	gi|9836652	Chromosome 20 open reading frame 3, C20orf3	37%/78	Exhibits strong arylesterase activity with beta-naphthyl acetate and phenyl acetate	Membrane
884	−0.68	gi|1705694	Cytochrome *c*-type heme lyase (CCHL), HCCS	22%/86	Links covalently the heme group to the apoprotein of cytochrome *c*	Mitochondrion inner membrane
1302	−0.66	gi|24475861	Phosphohistidine phosphatase 1, PHPT1	44%/186	EDTA-insensitive phosphohistidine phosphatase	Cytoplasm
664	−0.59	gi|38570107	EF-hand calcium binding domain 6, EFCAB6	20%/66	Negatively regulates the androgen receptor	Nucleus
709	−0.56	gi|62896663	Annexin A7, ANXA7	33%/292	Calcium/phospholipid-binding protein which promotes membrane fusion and is involved in exocytosis	Membrane binding
744	−0.49	gi|4502923	Calponin 3, acidic, CNN3	28%/74	Thin filament–associated protein	—

*Master spot ID is the unique master number that refers to the labels in Figure 1*B*.

†Fold change presents the ratio of miRNA-122 inhibitors to controls.

‡Accession no. is the MASCOT results of MALDI-TOF/TOF searched from the NCBInr database.

§Coverage (%) means the number of amino acids spanned by the assigned peptides divided by the sequence length. Protein score (based on combined MS and MS/MS spectra). The proteins had statistically significant protein score of great than 64 ($P \leq .05$) were considered successfully identified.

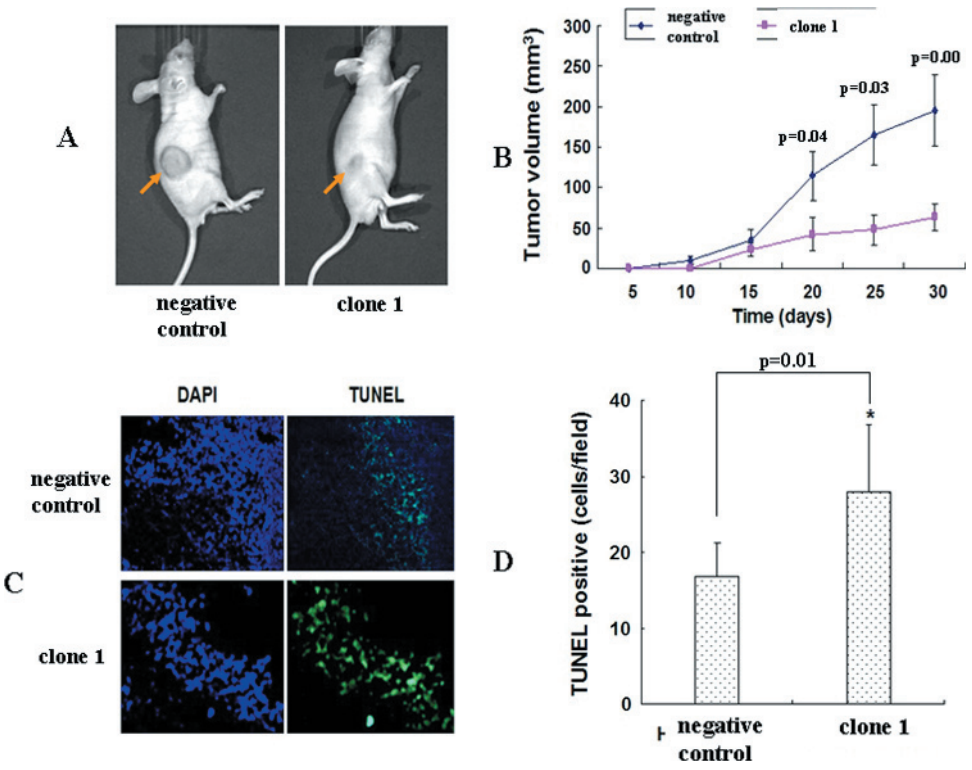

Figure W1. Subcutaneous tumors in nude mice. (A) The effects of miR-122 overexpression on subcutaneous tumors in nude mice. The arrows indicate the morphology of the tumors from the injected site. (B) *In vivo* subcutaneous tumor growth curves of stably transfected miR-122 or control HepG2 cells ($n = 5$, $^*P < .05$). The subcutaneous tumors were examined every five days after cell injection. Note that tumors that are induced by miR-122–transfected HepG2 cells are significantly reduced in size compared to that in the control. (C) The TUNEL results showed that the frequency of apoptotic cells is significantly increased in HepG2–miR-122 tumors. One of the representative fields is shown. (D) The number of TUNEL-positive cells per field was calculated ($n = 5$, $^*P < .05$).